UNIZIK JOURNAL OF ENGINEERING AND APPLIED SCIENCES (UJEAS)

Research Article

Perspectives of Coagulation for the Removal of Contaminants from Pharmaceutical Wastewater utilizing cucurbita seed as bio-coagulant

Collins N. Oguanobi, Okechukwu D. Onukwuli, Joseph O. Ezeugo.

Special Issue
A Themed Issue in Honour of Professor Onukwuli Okechukwu Dominic (FAS).

This special issue is dedicated to Professor Onukwuli Okechukwu Dominic (FAS), marking his retirement and celebrating a remarkable career. His legacy of exemplary scholarship, mentorship, and commitment to advancing knowledge is commemorated in this collection of works.

Edited by
Chinonso Hubert Achebe PhD.
Christian Emeka Okafor PhD.

UJEAS

UNIZIK JOURNAL OF ENGINEERING AND APPLIED SCIENCES

UNIZIK Journal of Engineering and Applied Sciences 4(2), March (2025), 1826-1840
Journal homepage: https://journals.unizik.edu.ng/index.php/ujeas
PRINT ISSN: 2992-4383 || ONLINE ISSN: 2992-4391

Perspectives of Coagulation for the Removal of Contaminants from Pharmaceutical Wastewater utilizing cucurbita seed as bio-coagulant

Collins N. Oguanobi[1*], Okechukwu D. Onukwuli[2], Joseph O. Ezeugo[3].

[1]Chemical Engineering Department, Michael Okpara University of Agriculture Umudike, Abia State Nigeria.

[2]Chemical Engineering Department, Nnamdi Azikiwe University Awka, Anambra State Nigeria.

[3]Chemical Engineering Department, Chukwuemeka Odimegwu Ojukwu University, Anambra State Nigeria.

[*]Corresponding Author's E-mail: oguanobi.nonso@mouau.edu.ng

Abstract
Pharmaceutical effluent is a hazardous waste of environmental concern due to the complex nature of its chemical composition. This research focused on using coagulation techniques to remove contaminants from aqueous solution via investigating the coagulation qualities of cucurbita seed on removal of total suspended solid (TSS), color, chemical oxygen demand (COD), and turbidity from pharmaceutical effluent. The batch system was applied to evaluate the effect of process-independent variables on the coagulation process. The coagulation kinetics were investigated using first-order and second-order kinetic expressions. The optimum removal efficiency of contaminants was predicted using the response surface methodology (RSM) model. The batch study results show maximum color and turbidity removal of 77% and 68% at pH 6, whereas COD and TSS removal is 55% and 60% at pH 8. The results also confirm the process to be dependent on coagulant dosage, reaction time, mixing speed, settling time, and temperature. The concordance RSM model's actual optimum color removal efficiency of 97.99% and R^2 of 0.9914 with the model's predicted removal efficiency of 97.63% and predicted R^2 of 0.9298 thereby indicate the accuracy of the model prediction. These obtained results confirm cucurbita seed as a reliable, cost-effective alternative coagulant for contaminant removal from pharmaceutical effluents.

Keywords: coagulation, cucurbita, kinetics, optimization, turbidity.

1. Introduction

Environmental contamination is the release of harmful substances or energies into the natural environment, leading to adverse effects on ecosystems and human health. These contaminants can be chemical agents, biological entities or physical factors. Pollution specifically, refers to the introduction of substances or forms of energy into the environment at a pace that exceeds the natural processes of dispersion, dilution, decomposition, recycling, or safe storage. The foundation of global environmental pollution lies in human actions associated with modernization and industrialization. Pollutants are generally categorized into three main types based on the affected environment: water pollution, air pollution, and land pollution (Adebowale et al. 2008, Ivanova 2020). Water pollution is the release of harmful substances into groundwater, lakes, streams, rivers, estuaries, and oceans, to a degree that disrupts the beneficial uses of water or the ecological integrity of ecosystems. Various sources contribute to water pollution, including industrial discharge, domestic waste, improper solid waste disposal, decaying animals, agricultural runoff, and sedimentation. Industrial effluent is a significant contributor and consists of waste and by-products from diverse production sectors such as pharmaceuticals, heavy metals, textiles, oil refining, food and beverage processing, cement, chemicals, sugar, iron and steel, and dye production (Oguanobi et al. 2024a).

The pharmaceutical industry plays a crucial role in addressing global health challenges by developing medications that prevent, treat, and manage diseases and infections. The positive effects of pharmaceuticals extend beyond personal and public health to encompass economic growth and advancements in science. Nonetheless, it is vital to acknowledge the adverse impacts this industry can have on both humanity and the environment (Samal et al. 2022). A significant issue pertains to the environmental pollution generated during the production of active pharmaceutical ingredients and drugs, as well as in the handling of pharmaceutical products. The wastewater produced by these industries is often extremely hazardous and toxic, containing various pharmacological substances, solvents, reagents, heavy metals, and other harmful materials. The release of such effluents into the environment without adequate treatment poses severe risks to humans, photosynthetic organisms, and aquatic life that rely on water for survival. Consequently, managing pharmaceutical wastewater has become a pressing global and environmental issue due to the increasing demand for medications, which, in turn, has led to the expansion of the pharmaceutical industry (Samal et al. 2022).

Recently, various physical, biological, physico-chemical and chemical treatment techniques such as sonochemical degradation, coagulation and flocculation, adsorption, electrochemical removal, photochemical degradation, bio-degradation, membrane separation, and others have been explored to mitigate pharmaceutical wastewater and overall water pollution at its source. Although studies indicate that these methods often have limitations and cannot fully treat pharmaceutical effluents due to their complex compositions (Vijayan et al. 2022). Response Surface Methodology (RSM) is a mathematical modeling approach used to determine optimal operating parameters for processes. It facilitates the simultaneous assessment of process variables that influence outcomes, even when complex interactions are present. RSM typically requires a limited number of experimental runs to predict the best conditions. An objective of this project is to investigate the coagulation ability of cucurbita seed via removal of certain notable contaminants present in pharmaceutical effluents.

2.0 Materials and methods

The primary raw materials used are cucurbita seeds obtained from cucurbita fruit bought from Orie-ugba market in Umuahia South Local Government Area of Abia State, Nigeria, and real pharmaceutical effluent obtained from a pharmaceutical industry in Enugu State, Nigeria, while the secondary raw materials used were all of analytical grade and bought from Bridge Head Market in Onitsha, Anambra State. All the solutions used were prepared with distilled water.

2.1 Preparation of green coagulant

The seeds were cleaned, dried, and homogenized into powder and kept in an airtight jar. Oil was removed by soaking the pulverized sample with ethanol in a conical flask in a w/v ratio of 1:6 (100 g of meshed sample was dissolved with 600 ml of the ethanol) and vigorously stirring the mixture for 150 min with a magnetic stirrer. The mixture was then filtered with whatman filter paper no. 3; afterward, the residue was sun-dried for three days and stored in a desiccator until used.

2.2 Characterization

2.2.1 Determination of Fat Content.

Two grams of meshed cucurbita seed sample was weighted and soaked with diethyl ether and allowed for 2 hours without stirring for complete reaction and sedimentation and dried at 50°C for 24 h. The fat content of the raw sample is determined using Equation 1:

$$\% Fat = \frac{Weight\ of\ fat\ X\ 100}{Weight\ of\ sample} \quad (1)$$

2.2.2 Determination of Protein Content.

The protein content was determined by the Kjeldahl three-step approach; digestion, distillation, and titration accordily. This Kjeldahl method gives quantification of nitrogen, and then the Nitrogen content is multiplied by a conversion factor of 6.25, to give protien content.

Protein content = Nitrogen content in sample $*$ 6.25.

2.2.3 Determination of Moisture Content

5 g of the cucurbita seed sample was measured, and the weight was noted as W_1. The weighted sample was then put in an oven and allowed to dry at 120°C for 2 hours, after which the dried sample was measured again and the weight noted as W_2. The moisture content is then expressed as a percentage using the formula of Equation 2.

$$\%\, moisture = \frac{W_1 - W_2}{W_1} \times 100 \quad (2)$$

2.2.4. Determination of Ash Content

5 g of cucurbita seed sample was measured and the weight noted before ashing. The ash content of the samples was calculated in relation to the dry weight of the original sample after 4 hr ignition of the sample at 650°C using furnace. The ash content of the samples was determined by the formula of equation 3:

$$\%\, Ash = \frac{Weight\ of\ ash\ X\ 100}{Weight\ of\ sample} \quad (3)$$

2.2.5 Determination of functional groups, surface morphology, and structural properties

The Cucurbita seed samples were analyzed to determine the functional group present and observe surface morphologies and structural properties. The functional group analysis is also called Fourier transform infrared (FTIR) analysis, and it was carried out using the Shimadzu spectrophotometer model S8400 with samples prepared by the conventional KBr disc method. The surface morphology analysis is also called scanning electron microscope (SEM) analysis, and it was carried out using the Joel scanning electron microscope model JSM 6400 with a coated gold film of layers approximately 20–25 A thick. The structural properties analysis is also called X-ray Diffraction (XRD) analysis, and it was carried out using a Power X-ray diffractometer with Kα radiation, which records the diffraction spectra.

2.3 Batch Coagulation/Flocculation Studies

In this study, coagulation/flocculation experiments were conducted using batch studies. Batch coagulation/flocculation experiments were conducted to investigate the process parametric effects of rapid mixing, slow mixing, stirring speed and contact time, pH, and temperature on wastewater contaminants (COD, TSS, color, and turbidity) uptake on cucurbit seed biocoagulant. Six beakers were assembled in the jar test apparatus, each containing 300 mL of real pharmaceutical wastewater. Hydrogen chloride (HCl) and sodium hydroxide (NaOH) were utilized to control the pH values during the study. Measurements of COD, TSS, color, and turbidity of the pharmaceutical wastewater sample were applied and taken as a reference to determine the capacity of the coagulant. The resulting effect of the studied process variables on real pharmaceutical wastewater contaminants uptake was determined using a turbidity meter for turbidity removal, a colorimeter for color removal, a spectrophotometer for TSS removal, and a chemical oxygen demand analyzer for chemical oxygen demand (COD) removal.

2.3.1 Mathematical method of analysis

Percentage contaminant removal efficiency was evaluated using Equation (4).

$$\text{Coagulation efficiency} = \varepsilon = \frac{(C_o - C_t)}{C_o} \times 100 \quad (4)$$

At equilibrium, contaminant removal "qe" (mg g^{-1}), was evaluated using expression of Equation (5)

$$qe = \frac{(C_o - C_e)V}{m} \quad (5)$$

Where C_o and C_e (mg L^{-1}) were initial and equilibrium concentrations respectively, C_t (mg L^{-1}) contaminant concentration at any time t while V and m were the volume of the solution in liter and the mass of dry sorbent used in gram. In kinetic experiments, aqueous samples were taken at different settling time intervals to determine the uptake of contaminant at any preset time t. Kinetic study is very important because the rate of contaminant removal from the effluent depends on the kinetic parameters (n and k). The rate equation contains an independent variable (t), a dependent variable (C), and kinetic parameters.

$$\frac{dC}{dt} = -KC^n \quad (6)$$

Rephrasing Equation (6) gives

$$RC = -KC^n \quad (7)$$

Where$\frac{dC}{dt} = RC$, C represents the concentration of particles, t is the coagulation time, k represents the nth order coagulation rate constant, and n is the order of the coagulation process.

The particle concentration is indirectly proportional to time. The rate of contaminant removal can be directly proportional to the amount of contaminant concentration absorbed by the coagulant used. The rate constant (K) is an outcome of the product of collision efficiency (ε) and the Smoluchowski rate constant for a quick coagulation process (K_{SRC}) (Sibiya et al. 2021).

$$K = \varepsilon \, X \, K_{SRC} \quad (8)$$

Where K_{SRC} is given by Equation (9)

$$K_{SRC} = \frac{4K_B T}{3\mu} \quad (9)$$

Where μ is the viscosity of the fluid.

$$\mu = \frac{K_B T}{6\pi D_B r} \quad (10)$$

Where r = particles radius

The Brownian diffusion coefficient (D_B) is given by Equation (11)

$$D_B = \frac{K_B T}{\beta} \quad (11)$$

Where β = the friction factor (m^3 kg/s)

$$\beta = 6\pi\mu r \quad (12)$$

The relationship between friction factor (β) and nth order coagulation rate constants calculated by

$$\beta = 2K \quad (13)$$

For the first order reaction (n = 1), Equation (3) becomes (14) when integrated:

$$\ln\frac{C_O}{C} = K_1 t \quad (14)$$

where C_O and C represent the initial and final concentration (mg/L) of flagyl and levofloxacin at t and K_1, which is the first order rate constant in l/min. A plot of $\ln\frac{C_O}{C}$ versus t will yield a straight line passing through the origin with a slope of K_1 using Equation (14) (Varsani et al. 2022). Nevertheless, if the line does not cross the origin but goes through another y-intercept, it obeys the second order coagulation process (n = 2) where Equation (6) becomes Equation (15):

$$\frac{dC}{dt} = -KC^2 \quad (15)$$

Then, Equation (15) yields Equation (16) after integration:

$$\frac{1}{C} = K_2 t + \frac{1}{C_0} \quad (16)$$

Rearranging Equation (16) to calculate the second order kinetic K_2 rate gives Equation (17),

$$K_2 = \frac{\frac{1}{C} - \frac{1}{C_O}}{t} \quad (17)$$

Where K_2 is the pseudo-second order coagulation rate constant($L\, mg^{-1}\, min$)and the aggregations of coagulating particles generally follow the second order kinetics model.

Half-life period ($t_{1/2}$) is the time required for the initial level of flagyl and levofloxacin to reduce to one-half of the original value. The half-life period for the pseudo first-order kinetic is calculated by Equation (18) (Varsani et al. 2022).

$$t_{1/2} = \frac{\ln 2}{k} \quad (18)$$

The half-life period for the pseudo - second order kinetic is calculated as per Equation (19);

$$t_{1/2} = \frac{1}{kC_o} \quad (19)$$

3.0 Result and Discussion

Design expert version 13 was used in both the design and the RSM-CCD analysis. The experiment was designed using a central composite design (CCD) with five factor levels. RSM uses data obtained from design of experiments and statistical modeling technique to solve multi-variant problems (Venkatesh and Karthikeyan 2018; Oguanobi et al. 2024c). The independent variables used were pH, coagulant dosage, and settling time while the actual response (removal efficiency) was the dependent variable. The number of data sets for RSM-CCD experiment can be evaluated using expression of Equation 20.

$Q = 2^q + 2q + q_c$ (20)

Where q is the number of input factors and 2^q, 2q and q_c represents the: factorial points, axial points, and center points. The link between the process variables and dependent variables was estimated using second-order polynomial as in Equation 21 (Onukwuli et al. 2021).

$$R = \beta_o + \sum_{i=1}^{k} \beta_i \alpha_i \ldots\ldots + \ldots \sum_{i=1}^{k} \beta_{ii} \alpha_i^2 \ldots\ldots + \cdots \sum_{i=1}^{k-1} \sum_{j=1}^{k} \beta_{ij} \alpha_i \alpha_j \quad (21)$$

Where R is the calculated response, β_o is the model constant, β_i, β_{ii} and β_{ij} are the calculated coefficients second-order polynomial expression for the linear, quadratic and products of α_i, α_i^2 and $\alpha_i \alpha_j$, respectively.

3.0 Results and Discussion

3.1 Characterization Result

The proximate analysis of the Cucurbita seed was carried out to determine the physical properties and other characteristics of the bio-coagulant. Moisture content increases as the temperature and the duration of drying increase. Since the moisture content is an indication of the water activity, it thereby measures the stability and vulnerability to microbial infection (Gado et al. 2017). The result of the moisture content of 4.96% is low, which is an indication that the materials have storage advantages (Mohaammed et al. 2014). Fats are necessary for the structural and biological functions of cells and aid in the transportation of fat-soluble vitamins, which are necessary for proper nutrition. The result of a fat content of 41.3% implies that the fat content of cucurbita seed samples is high, and this means that cucurbita seeds can serve as an energy-dense food, but on the other hand, the shelf life and spoilage rate of the sample can be affected because the fats can become rancid over time.

The ash content of a sample gave insight on the composition, properties, and quality of the samples. The results of the ash content of 0.66% imply that there is a significant concentration of different mineral elements in cucurbita, which should enhance growth and development and speed up metabolic processes (Elinge et al. 2012). This low obtained value suggests that the sample is free from contaminants with dirt, dust, or other impurities. Proteins are complex biological molecules made up of amino acids supporting growth and development. The results of the protein content of 37.62% showed that the protein content of the **C**ucurbita seed samples is moderate. This moderate protein content of cucurbita seed shows that it can serve as a source of protein for animal feed formulation in animal nutrition (Kwiri et al. 2014, Falaye and Sule 2020). The moderate protein content can as well affect the stability and shelf life of the material over time because protein can denature or degrade.

3.1.1 FTIR analysis

Fig. 1a and b present the FTIR spectra of raw cucurbita seed (RCS) and sludge after coagulation (SC). The FTIR analysis was used to examine the surface functional groups of the coagulant and to identify those groups responsible for contaminant removal. Adsorption in the IR region takes place because of rotational and vibrational movements of the molecular groups and chemical bonds of a molecule (Kakkar et al. 2014). The IR of the raw cucurbita sample is characterized by enough oxygen-containing functional groups, such as carboxyl and hydroxyl groups (O-H, C-O, C=O bond), which are responsible for the binding of contaminants to the coagulant. The peak at wavenumber 3276.3 in the spectra signals the presence of O-H and NH-group which is a neutral compound and easily gets protonated in the acidic solution and as well support adsorption. The peak at wavenumber 2855.1-2134.6 in the spectra signals the presence of C=O stretch of the carboxyl group. The IR characteristic peaks of amide I between 1700–1600 cm^{-1} and amide II between 1560–1500 cm^{-1} weave numbers also support the binding of contaminants on the coagulant. The peak at wavenumber 1100-1300 in the fingerprint region of the spectra signals the presence of C-O stretch of the carboxyl group and can also support the binding of contaminants on the coagulant. The IR of the

sludge shows a reduced number of peaks, a change in the peak intensity, and a shift in the wave numbers, which is a good indication that coagulation and adsorption have taken place. These may be attributed to the interaction of the solute with functional groups on the surface of the coagulant.

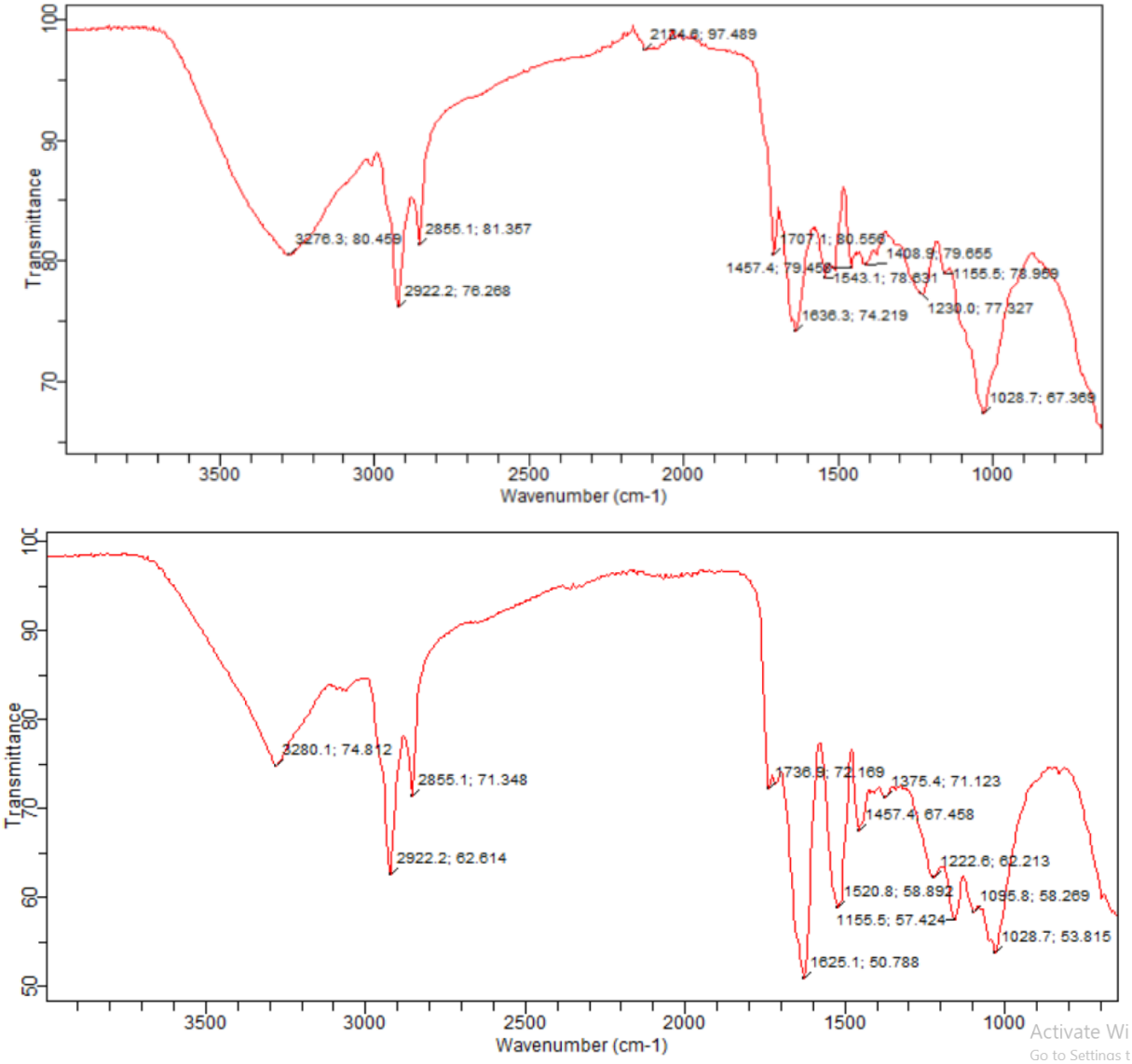

Figure 1: FTIR spectra of: (a) raw cucurbita seed (RCS), (b) sludge after coagulation (SAC).

3.1.2 SEM micrographs

Figures 2a and b present the scanning electron micrograph (SEM) of raw cucurbita seed (RCS) and sludge after coagulation (SAC), respectively. The micrograph of Figure 2a clearly displayed a considerable number of heterogeneous layers of pores and an internal surface of the Cucurbita seed material, whereas the EDX presented the table of elemental content of the sample. From the table, the presence of aluminum, silicon, and calcium was observed in the sample, and these elements support coagulation through charge neutralization, bridging, and precipitation of soluble contaminants of the effluent. Figure 2b presents the micrograph of the sludge sample, and from the EDX, it's seen that the atomic concentrations of aluminum, silicon, and potassium increase, and the presence of oxygen was observed. These outcomes show that the sample was able to precipitate out the elemental content of the wastewater.

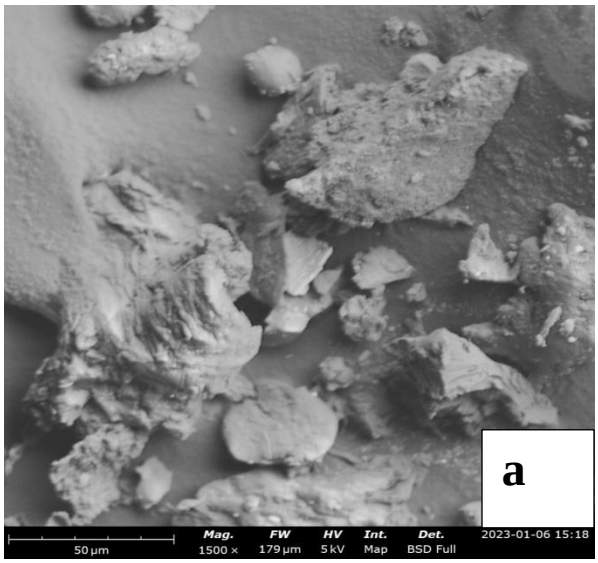

Element Number	Element Symbol	Element Name	Atomic Conc.	Weight Conc.
6	C	Carbon	75.40	70.40
7	N	Nitrogen	22.27	24.25
13	Al	Aluminium	0.34	0.74
15	P	Phosphorus	0.19	1.16
19	K	Potassium	0.30	0.91
12	Mg	Magnesium	0.35	0.67
16	S	Sulfur	0.21	0.51
14	Si	Silicon	0.15	0.33
11	Na	Sodium	0.17	0.31
17	Cl	Chlorine	0.10	0.27
20	Ca	Calcium	0.00	0.00
22	Ti	Titanium	0.00	0.00
26	Fe	Iron	0.00	0.00

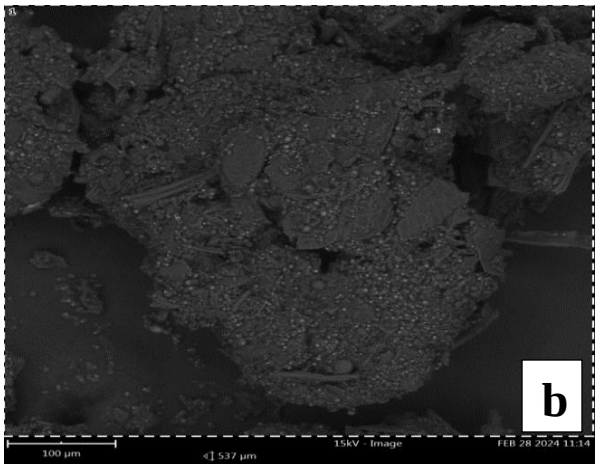

Element Number	Element Symbol	Element Name	Atomic Conc.	Weight Conc.
6	C	Carbon	97.85	94.61
17	Cl	Chlorine	0.52	1.47
16	S	Sulfur	0.39	1.01
13	Al	Aluminium	0.57	1.19
14	Si	Silicon	0.22	0.50
15	P	Phosphorus	0.48	0.47
22	Ti	Titanium	0.11	0.44
11	Na	Sodium	0.21	0.38
12	Mg	Magnesium	0.15	0.29
19	K	Potassium	0.03	0.09
20	Ca	Calcium	0.00	0.00
26	Fe	Iron	0.00	0.00

Figure 2. SEM Micrograph of: **(a)** raw cucurbita seed (RCS) **(b)** sludge after coagulation (SAC)

3.1.3 X-ray diffraction (XRD)

X-ray diffraction is a common technique that determines the structure of atoms within the sample, whereas for small crystal sizes, it determines sample composition, crystallinity, and phase purity. XRD data (intensity vs. 2 theta) gives a lot of information about why some peaks are of high and low intensity. Peak intensity represents the atomic position in the crystal structure; for instance, some peaks are high in intensity due to the fact that there is more periodicity than in the other directions.

From Figure 3, it is seen that the spectra are characterized by broad, sharp, high, and low-intensity peaks, which is to say that cucurbita seed sample is made up of both crystalline and amorphous structures. The presence of broad peaks signals amorphous structure, whereas the presence of sharp peaks signals crystal structure. The figure also shows that cow hoof exhibit more crystalline structure than amorphous structure, which plays a vital role in enhancing the rate of coagulation. Crystalline surfaces exhibit high: surface charge, surface roughness, and surface energy, which attracts and bind opposite charged particles, provide habitat for particles to aggregate and coagulate, and derive the adsorption of particles.

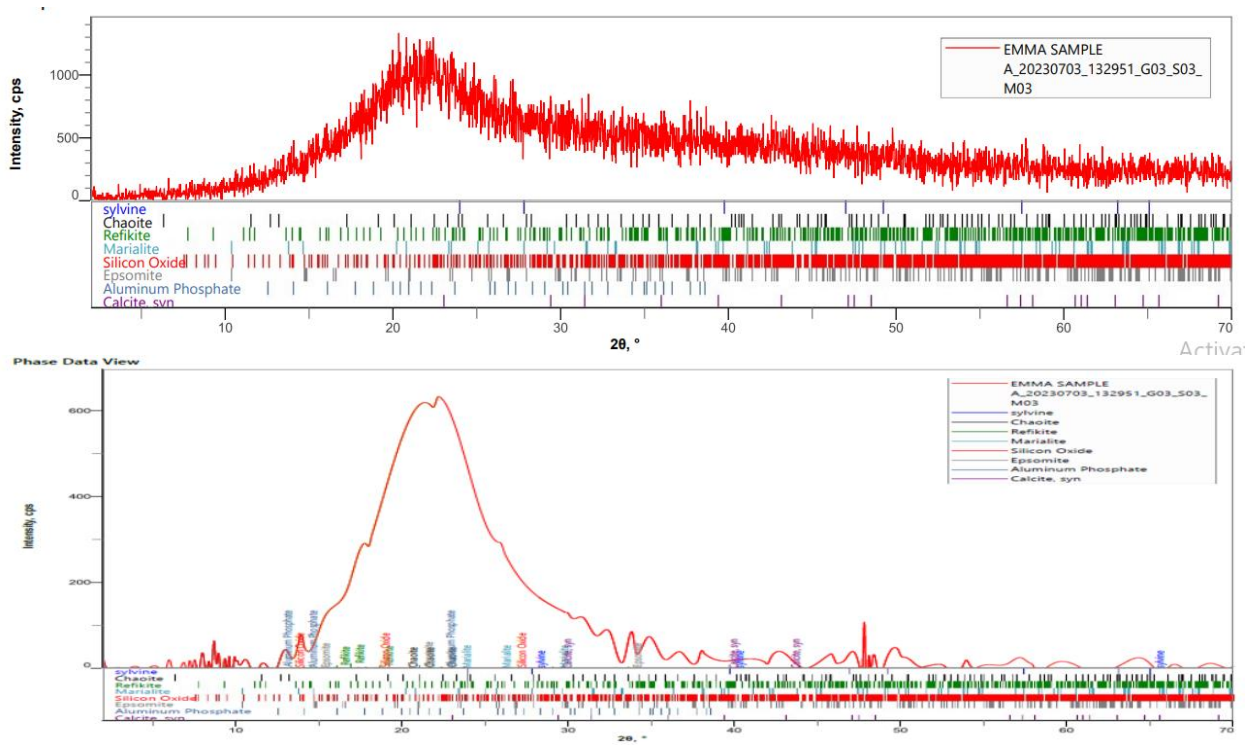

Figure 3: XRD of cucurbita seed

3.2 Batch coagulation result

3.2.1 Effect of coagulant dosage

The effect of coagulant dosage was studied at the dosage range of 0.3, 0.7, 1, 1.3, and 1.7 g/l of real pharmaceutical effluent of unknown concentration at a constant temperature of 313 K, a pH of 6 and 8, a reaction time of 30 min, and a settling time of 60 min. The result of the study, as seen from Figure 4a, shows that the percentage removal of color and turbidity increases from 66.05 to 88.55% and from 63.85% to 81.34%, respectively, with an increase in coagulant dosage from 0.3 g/l up to the optimum dosage of 1 g/l and thereafter decreases at further dosage increase to 1.3 g/l. The subsequent observed decrease in percentage removal at 1.3 g/l and 1.7 g/l dosage is attributed to over-dosage, which creates excess H+ at the coagulant surface, thereby causing electrostatic repulsion among the particles or re-stabilizing the particles (Hassan et al., 2009), whereas removal of COD and TSS increases from 37.65 to 77.41 and from 35.71 to 74.00%, respectively, with an increase in coagulant dosage from 0.3 g/l to a dosage of 1.7 g/l. A similar result of the same trend was reported on the coagulation/flocculation process for textile mill effluent treatment (Karam et al. 2020).

3.2.2 Effect of pH

The solution pH is important when the surface charge of coagulants and stabilization of the suspension are capable of ionizing in response to pH. The effect of pH on the percentage removal efficiency of real pharmaceutical effluent contaminants was studied at pH ranges of 2, 4, 6, 8, and 10, at a constant temperature of 313 K, a reaction time of 30 min, a settling time of 60 min, and an adsorbent dosage of 1 g/L for color and turbidity, whereas a 1.7 g/L optimum dosage was used for COD and TSS. The result of the study, as reported in Figure 4b, shows that the optimum removal of 78.65% and 61.04% for color and turbidity, respectively, was achieved at pH 6, whereas the optimum removal of 60.72% and 58.22% was recorded at pH 8 for COD and TSS, respectively. The optimum removal efficiency of color and turbidity at pH 6 is due to the very low solubility of color at pH < 6. Acidic pH leads to an increase in H^+ ion concentration in the system, and the neutral functional groups of amine (NH_2) in the cucurbita seed surface acquire positive charge by adsorbing H^+ ions. The maximum removal efficiency of COD and TSS is achieved around pH 8. At lower pH < 8, the number of positively charged surface sites of the functional groups on cucurbita seed increases, which does not favor the coagulation of cationic solution due to electrostatic repulsion. The decrease of percentage removal at alkaline medium > pH 8 may be due to a high rate of OH^- ions, which collide with the negative and neutral functional groups of the bio-coagulant, thereby causing electrostatic repulsion. A

similar result of the same trend was reported on the coagulation/flocculation process for textile mill effluent treatment (Karam et al. 2020) and on the use of Aloe vera as an organic coagulant for improving drinking water quality (Benalia et al. 2021).

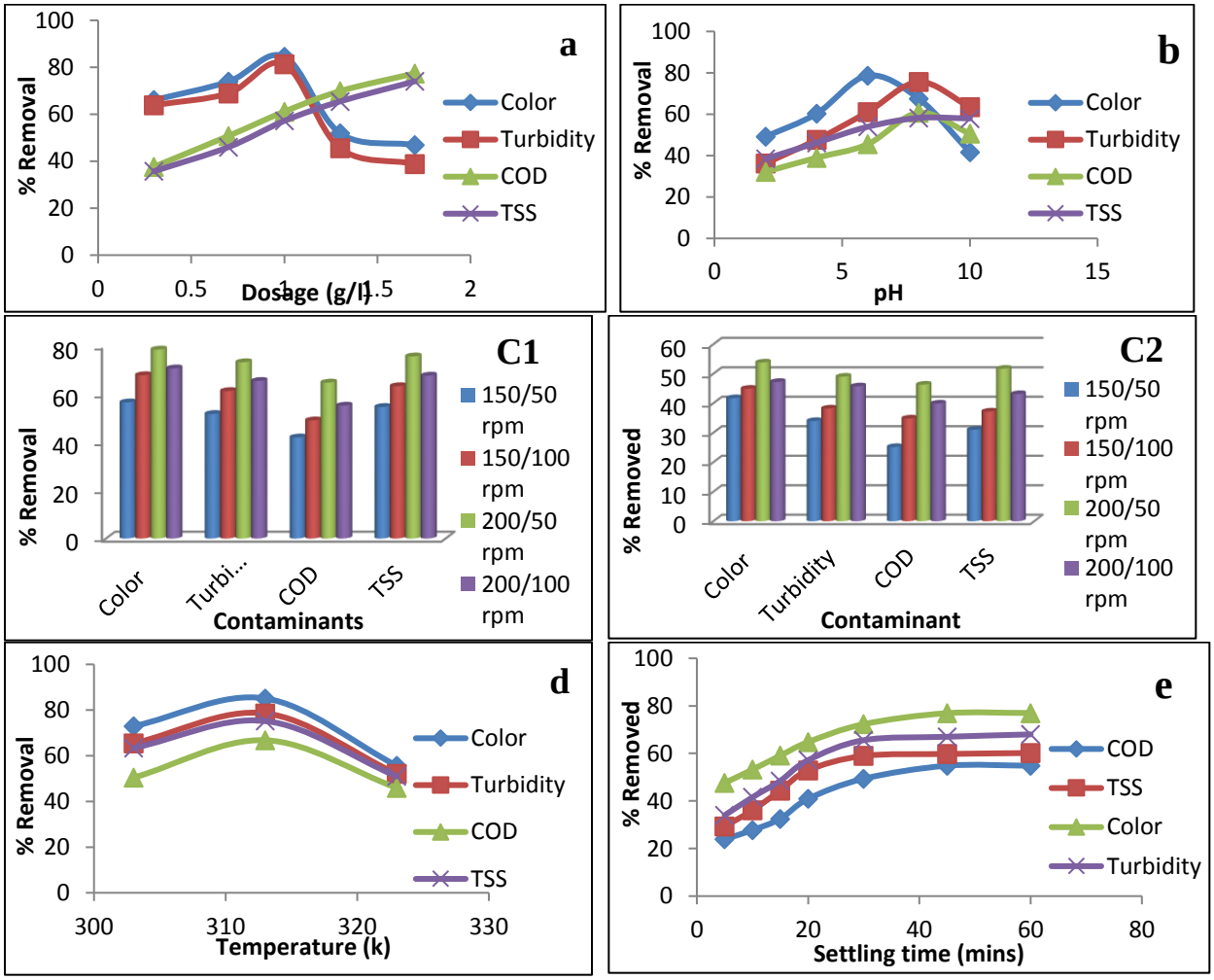

Figure 4: Effects of process parameters displaying impact of (a) coagulant dosage, (b) pH, (c) stirring speed, (d) temperature, and (e) settling time

3.2.3 Effect of mixing speed

The effect of mixing speed and time is crucial for the formation and growth of flocs. The impact of mixing speed and time was examined at the combined effect of rapid and slow mixing together (150/50 rpm, 200/50 rpm, 150/100 rpm, 200/100 rpm) at time ratios of 5:25 mins and (150/50 rpm, 200/50 rpm, 150/100 rpm, 200/100 rpm) at time ratios of 25:5 mins, at a temperature of 313K, a coagulant dosage of 1 g/l, a pH of 6 for color and turbidity and pH 8 for COD and TSS, and a settling time period of 60 minutes. The results of the study as reported in Figures 4C1 and C2 show a high removal capacity of 78.39%, 73.14%, 64.69%, and 75.55% for color, turbidity, COD, and TSS, respectively, at 5 minutes of rapid and 25 minutes of slow mixing, whereas a high removal capacity of 53.84%, 49.02%, 46.32%, and 51.73% for color, turbidity, COD, and TSS, respectively, at 25 minutes of rapid and 5 minutes of slow mixing. The obtained result showed that 5 minutes of rapid and 25 minutes of slow mixing are more effective than 25 minutes of rapid and 5 minutes of slow mixing. The 5 minutes of rapid mixing is attributed to a high-intensity, short-duration mechanism that promotes flocculant dispersion and henceforth aids in fast charge neutralization, whereas 25 minutes of slow mixing is attributed to low-intensity, long-duration mixing, which promotes floc formation and consolidation for high coagulation efficiency. The similar result of the same trend was reported on challenges and opportunities of biocoagulant/bioflocculant application for drinking water and wastewater treatment (Kurniawan et al. 2020).

3.2.3 Effect of Temperature

Temperature studies the adsorption thermodynamics and nature. The impact of temperature on contaminant removal was examined at temperature ranges of 303 K, 313 K, and 323 K at a constant coagulant dosage of 1 g/l for color and turbidity, whereas a 1.7 g/l optimum dosage was used for COD and TSS, a pH of 6 for color and turbidity and pH 8 for COD and TSS, a time period of 30 minutes (5 mins rapid mixing at 200 rpm and 25 mins slow mixing at 50 rpm), and a settling time period of 60 minutes. The result of the study, as reported in Figure 4d, shows an increase in removal efficiency of contaminants from 72.9% at 303 K to 85.1% at 313 K, 65.4% at 303 K to 78.6% at 313 K, 50.4% at 303 K to 66.8% at 313 K, and 63.4% at 303 K to 75.2% at 313 K for color, turbidity, COD, and TSS, respectively, as the temperature of the solution increases. This outcome confirms the contaminants removal from real pharmaceutical effluent using a biocoagulant as an endothermic system. The observed increase in contaminant uptake is as a result of an increase in the mobility and kinetic energy of molecules, which may also cause enlargement and disintegration of the internal structure of the coagulant, thereby enabling large contaminant molecules to penetrate further. Moreover, the result of the study, as in Figure 4d, also shows a decrease in the removal efficiency of contaminants as the solution temperature increases to 323 K. This is attributed to the degradation or breakdown of coagulant functional groups at higher temperatures, which negatively influence**s** coagulant performance and effectiveness. The obtained result is in harmony with the previous report by Othman et al. (2008).

3.2.5 Effect of settling time

The effect of settling time was studied at sedimentation times ranging from 5 to 60 mins, and results are shown in Figure 4e. The result shows an increase in the amount or percentage of removal as settling time increases from 5 to 60 minutes. This is attributed to orthokinetic coagulation, which allows longer settling times for better floc formation. The similar result of the same trend was reported on coagulation treatment of wastewater: kinetics and natural coagulant evaluation (Sibiya et al. 2021).

3.3 Kinetic Modeling

Coagulation kinetics refers to the study of the mechanism and rate (how fast or slow) at which molecules and particles agglomerates to form flocs. For evaluating the coagulation kinetics of the studied contaminant onto cow hoof, first-order and second-order kinetic models were used to fit the experimental data. A plot of $\ln\frac{C_O}{C}$ versus t will yield a straight line passing through the origin with a slope of K_1 (Varsani et al. 2022). Nevertheless, if the line does not cross the origin but goes through another y-intercept, it obeys the second order coagulation process. The curve fittings of the models are presented in Figure 5. The values of the respective constants of the model were evaluated and tabulated in Table 1.

The first-order model equation is used to test the experimental data and thus to explain the coagulation kinetics. Plots of ln(Co/C) against t were used to express the first-order kinetic process at 313K temperatures. From the result of Figure 5a, it's seen that correlation coefficient R^2 values were 0.8935, 0.7648, 0.8995, and 0.8279 for COD, TSS, color, and turbidity, respectively. This indicates that the coagulation process may have followed the first-order kinetics model, but since the Y-axis intercepts are not in accordance with the first-order kinetic equation, the kinetic reaction process is confirmed to be the second-order coagulation process. The high obtained values of the coagulation rate constant (K), as seen in Table 1 for the contaminants, signify fast coagulation, good floc formation, optimal coagulation conditions, and efficient coagulant.

Figure 5b presents the plot of 1/C versus t, which demonstrates the second-order kinetic model. The values of second-order kinetic parameters were presented in Table 1. The correlation coefficient R^2 values of 0.9133, 0.7963, 0.9301, and 0.8637 for COD, TSS, color, and turbidity, respectively, were obtained. High values of R^2 indicate a great level of linearity, accuracy, and effectiveness of the equation in describing the coagulation-flocculation process. The significant values of obtained k_1 and k_2, as seen in Table 1 for the contaminants, are in concordance with the results of the coagulation rate constant (K). The high RC values, as in Table 1, indicate a high rate of contaminant reduction. The obtained significant K_{SRC} value of 0.879678 indicates a quick coagulation process, and this validates the results of the coagulation rate constant (K), first and second order rate constants

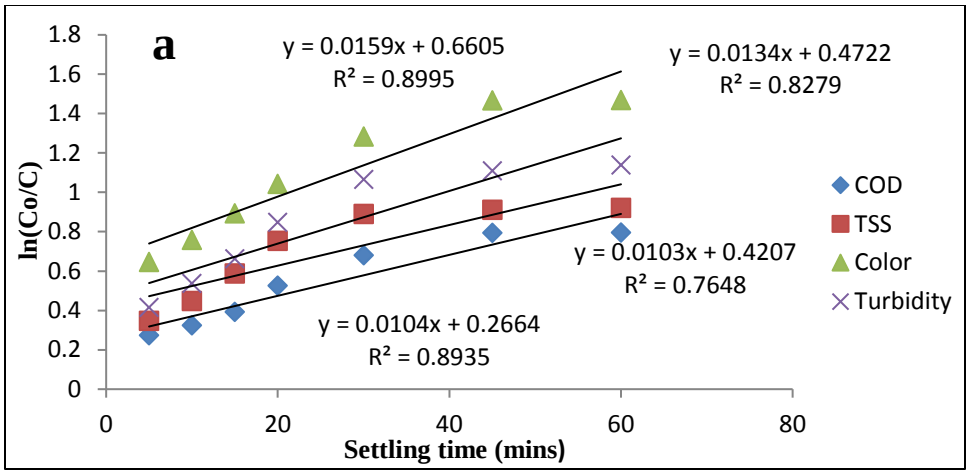

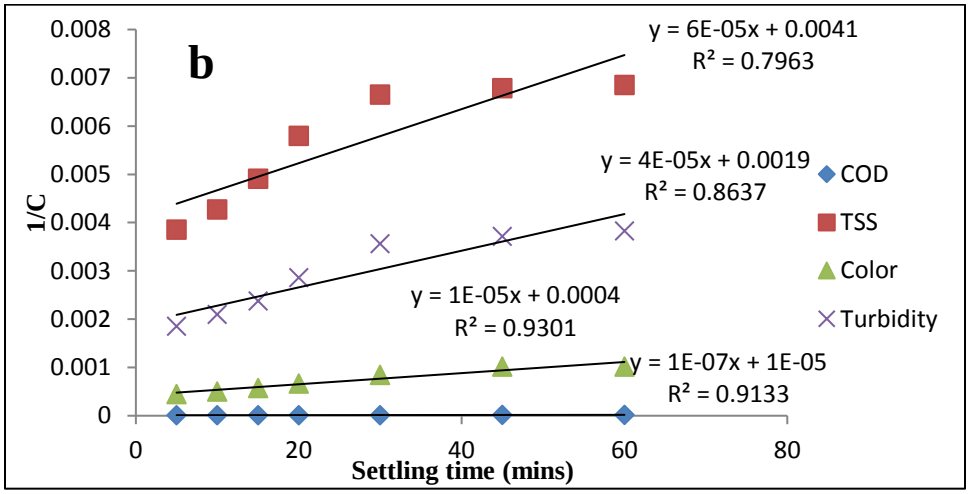

Figure 5. Kinetic plot for removal of contaminants using cucurbita biocoagulant

Table 1 Calculated kinetic parameters

Parameters	COD	TSS	Color	Turbidity
First order				
R^2	0.8935	0.7648	0.8995	0.8279
K_1	0.0104	0.0103	0.0159	0.0134
□	54.85	60.17	76.8	67.8
K_{SRC}	0.879678	0.879678	0.879678	0.879678
K	48.25035	52.93024	67.55929	59.64219
RC	4825.035	5293.024	6755.929	5964.219
$t1^{/2}$	0.014366	0.013095	0.01026	0.011622
Second order				
R^2	0.9133	0.7963	0.9301	0.8637
K_2	980.4303	2.431515	16.31394	4.347601
$t1^{/2}$	1.59E-07	5.16E-05	3.48E-06	2.06E-05
RC	8.19E+11	7101952	1.22E+09	39625554

3.4 Optimization Using Response Surface Methodology

ANOVA Analysis for turbidity Removal

Design expert was used to analyze the result and the summary of P-value and the model summary statistics are presented in Table 2.

Table 2: Statistical summary of the models investigated

Source	Df	Standard deviation	R-squared	Adjusted R^2	Predicted R^2	PRESS
Linear	11	6.04	0.0370	-0.1436	-0.4715	891.31
2FI	8	6.64	0.0533	-0.3836	-2.1351	1899.05
Quadratic	5	0.7213	0.9914	0.9837	0.9298	42.53
Cubic	1	0.7331	0.9947	0.9831	-1.2219	1345.90

The quadratic model for optimum point prediction of the process was suggested from the CCD module with high R-squared, adjusted R^2 and predicted R^2 values of 0.9914, 0.9837, and 0.9298 respectively. Analysis of variance (ANOVA) confirms the adequacy of the quadratic model.

Table 3: ANOVA and model coefficients for color removal

Source	Sum of squares	df	Mean squares	F-value	p-value Prob>F
Model	600.53	9	66.73	128.25	< 0.0001
A-Dosage	6.31	1	6.31	12.14	0.0059
B-pH	1.18	1	1.18	2.27	0.1627
C-Settling time	14.90	1	14.90	28.64	0.0003
AB	3.34	1	3.34	6.42	0.0297
AC	0.0903	1	0.0903	0.1736	0.6857
BC	6.46	1	6.46	12.42	0.0055
A^2	27.92	1	27.92	53.67	< 0.0001
B^2	0.5410	1	0.5410	1.04	0.3319
C^2	468.16	1	468.16	899.81	< 0.0001
Residual	5.20	10	0.5203		
Lack of fit	5.20	5	1.04		
Pure error	0.0000	5	0.0000		
Cor total	605.73	19			

Significant terms of the model are checked from F-values and P-values. The higher the F-value, the smaller the P-value, and the more significant the corresponding coefficient. The model F-value of 128.25 implies that the model is significant, and P-values less than 0.0500 indicate that the model terms that are significant; therefore, A, C, AB, BC, A^2, and C^2 are significant terms (Oguanobi et al. 2024b). The empirical correlation between the variables (response and independent) in the coded form on the basis of the significant terms of experiment results was reported as follows:

$$\text{Removal efficiency (\%)} = 79.93 + 0.7422A + 1.14C - 0.6462AB + 0.8988BC + 2.00A^2 + 8.20C^2 \quad (22)$$

The good fit of the model equation was validated using R^2 (coefficient of regression). The high coefficient of regression value of 0.9914 implies that 99.1% of the variability in the response can be explained by the model.

The equation in terms of actual factors can be used to make predictions about the response for given levels of each factor. Here, the levels should be specified in the original units for each factor. This equation should not be used to determine the relative impact of each factor because the coefficients are scaled to accommodate the units of each factor and the intercept is not at the center of the design space. The empirical correlation between the variables (response and independent) in the actual form was reported as follows:

$$\text{Removal efficiency (\%)} = +97.56892 - 5.51342\text{Dosage} + 0.044960\text{pH} - 0.230804\text{Settling time} - 0.230804\text{Dosage} * \text{pH} - 0.006071\text{Dosage} * \text{Settling time} + 0.008988\text{pH} * \text{Settling time} + 4.08549\text{Dosage}^2 - 0.017415\text{pH}^2 + 0.0131158\text{Settling time}^2 \quad (23)$$

3.4.1 RSM graphical plots

The plot of Figure 6 shows the relationship between the actual and predicted values of the response. The data were analyzed to examine the correlation between the experimental and predicted responses. As seen from the figures, the data points were well distributed along a straight line at an angle of 45°, which suggested an excellent relationship between the experimental and predicted values of the response, and this certifies the underlying assumptions of the above analysis as accurate. The results also indicated that the selected quadratic model was adequate in assuming the response variables for the experimental data.

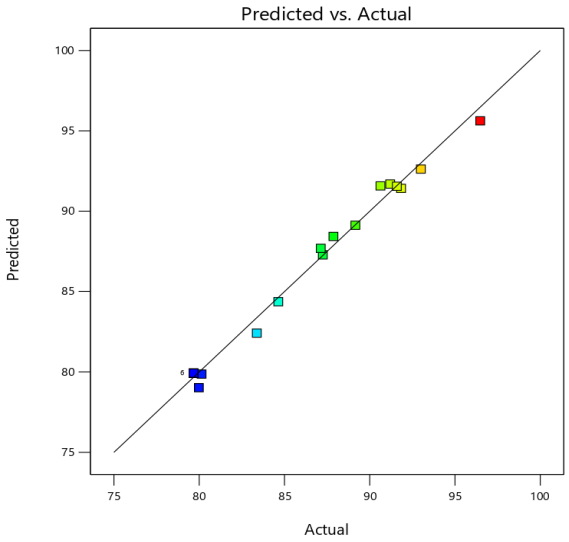

Figure 6 Plot of the experimental and predicted response

The 3D surface plots represent the effect of two process variables on the removal of colour. Figure 6a-c, presents the relationship between every two independent process variables.

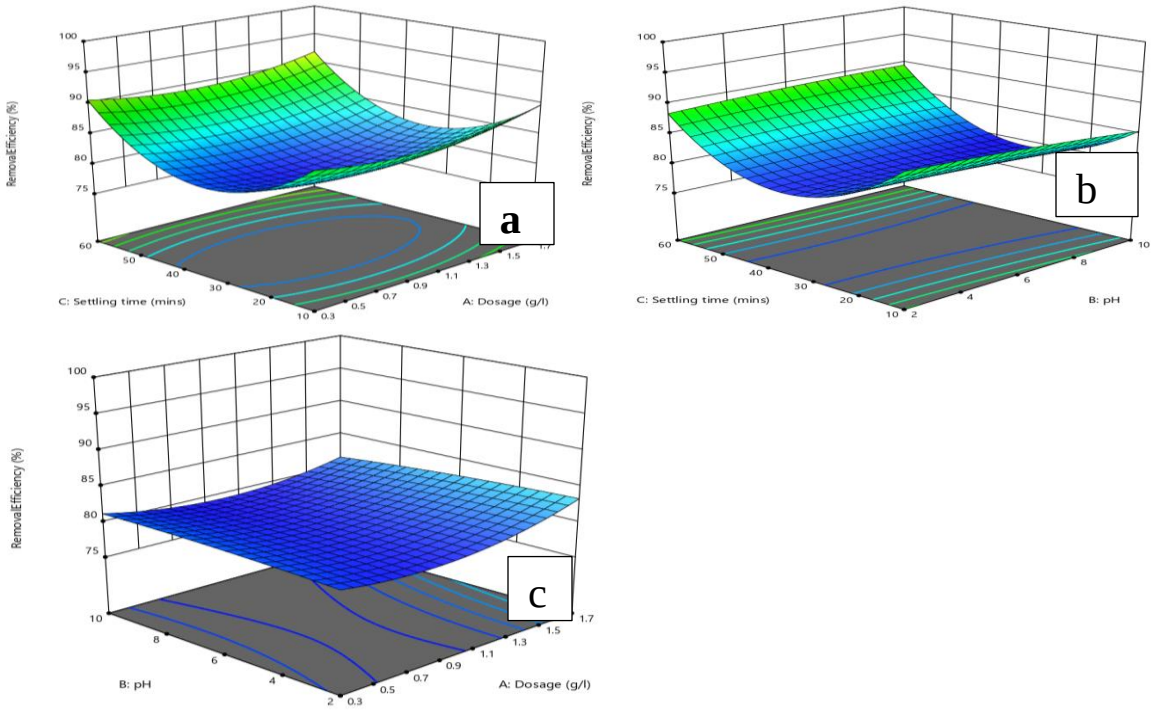

Figure 6. 3D surface plot for turbidity removal on the coagulant showing combined effects of (a) Settling time and Dosage, (b) pH and Settling time, and (c) Dosage and pH.

The ecliptic nature of the contour in the graph of figure 6a shows that there was a good significance between every two variables. The saddle nature of the contour in the graph of Figures 6b and c shows a complex and non-linear relationship between the variables. Moreover, figures 6a-c show that removal efficiency gradually and continuously increases as the variables increase.

4.0 Conclusions

The present study established the potential of cucurbita as a good coagulant for the removal of contaminants from aqueous solutions. The removal of COD, TSS, color, and turbidity from cucurbita was found to be dependent on the pH solution, temperature, coagulant dosage, contact time, settling time, and stirring speed. The coagulation kinetics is best described by a second-order kinetic model. The RSM prediction on turbidity removal was in concordance with the model's actual result and the one-factor-at-a-time result. Finally, further studies on the use of cucurbita to remove antibiotics from pharmaceutical effluent and exploring hybrid treatment systems combining cucurbita with other materials for coagulation systems or other technologies to improve their efficiency are recommended.

References

Adebowale K. O, Agunbiade F. O, and Olu-Owolabi , B. I. 2008 Impacts of Natural and Anthropogenic Multiple Sources of Pollution on The Environmental Conditions of Ondo State Coastal Water, Nigeria. EJEAFChe, 7 (4), 2008. [2797-2811]

Benalia, A.; Derbal, K.; Khalfaoui, A.; Bouchareb, R.; Panico, A.; Gisonni, C.; Crispino, G.; Pirozzi, F.; Pizzi, A. 2024 Use of Aloe vera as an Organic Coagulant for Improving Drinking Water Quality. Water 2021, 13,. https://doi.org/10.3390/w13152024

Elinge C. M., Muhammad A., Atiku F. A., Itodo A. U., Peni I. J., Sanni O. M., Mbongo A. N. 2012 Proximate, Mineral and Anti-nutrient Composition of Pumpkin (Cucurbitapepo L) Seeds Extract. *International Journal of Plant Research* 2012, 2(5): 146-150 DOI: 10.5923/j.plant.20120205.02

Falaye, A. E., and Sule, S. O. 2020. Chemical composition of differently processed Cattle Hoof meal Waste as Feedstuff Ingredient. Ukrainian Journal of Veterinary and Agricultural Sciences, 3(1), 47-51. https://doi.org/10.32718/ujvas3-1.09

Gado A. A, Falusi O. A, Adebola M. O, Gana, A. S, Muhammad L. M, and Abubakar A. 2017. Proximate and Mineral Analysis of Selected Cucurbita Species in Nigeria. *IJABR* Vol. 8(2): 192- 198

Hassan M, Tan P, and Noor Z, Z 2009. Coagulation and flocculation treatment of wastewater in textile industry using chitosan, Journal of Chemical and Natural Resources Engineering, Vol.4(1):43-53

Ivanova V. R 2020. The Anthropogenic Air Pollution And Human Health . Journal of IMAB - Annual Proceeding (Scientific Papers). 2020 Apr-Jun;26(2). DOI: 10.5272/jimab.2020262.3057

Kakkar P, Madhan B, Shanmugam G. 2014. Extraction and characterization of keratin from bovine hoof: A potential material for biomedical applications. Springerplus. 2014 Oct 10;3:596. doi: 10.1186/2193-1801-3-596.

Karam A, Emad S. B, and Zaher K. 2020 Coagulation/flocculation process for textile mill effluent treatment: experimental and numerical perspectives, International Journal of Sustainable Engineering, DOI: 10.1080/19397038.2020.1842547

Kurniawan S. B, Abdullah S.R. S, Muhammad Fauzul Imron M. F, Said N. S, M, Ismail N. I, Hasan H. A, Othman A. R, and Purwanti I. F 2020 Challenges and Opportunities of Biocoagulant/Bioflocculant Application for Drinking Water and Wastewater Treatment and Its Potential for Sludge Recovery Int. J. Environ. Res. Public Health , 17, 9312

Kwiri R, Winini C, Musengi A, Mudyiwa M, Nyambi C, Muredzi P, and Malunga A 2014. Proximate Composition of Pumpkin Gourd (Cucurbita Pepo) Seeds from Zimbabwe. International Journal of Nutrition and Food Sciences 3(3):279-283. DOI:10.11648/j.ijnfs.20140304.17

Mohaammed S. S, Paiko Y. B, Mann A, Ndamitso M. M, Mathew J. T, and Maaji S. (2014) Proximate, Mineral and Anti-nutritional Composition of Cucurbita Maxima Fruits Parts. *Nigerian Journal of Chemical Research* Vol. 19, 2014

Oguanobi N. C, Okonkwo. G, Onukwuli O. D, Ude C. N, Anike E. N. 2024b. Kinetic and Modeling of Anionic Dye Adsorption onto Acid modified Ihiala Clays: ANN, ANFIS and RSM comparative analysis. UNIZIK Journal of Engineering and Applied Sciences 3(2), June (2024), 608-613. Journal homepage: https://journals.unizik.edu.ng/index.php/ujeas

Oguanobi N.C, Ude C.N, Nnaji P.C, Onukwuli O.D, Anike E.N. Okonkwo. G, and Okonkwo C.H. 2024a. Adsorption Behaviors of Raw Clay for Cationic Dyes Removal: Equilibrium, Kinetic Modeling, Thermodynamics, and RSM Optimization, *Umudike Journal of Engineering and Technology*. vol. 10 No. 1, June 2024. Doi: https://doi.org/10.33922/j.ujet_v10i1_19.

Oguanobi N.C, Ude C.N, Onukwuli O.D, Anike E.N. Calistus N. Ude, Kalu C.B. 2024c. Adsorption Kinetics of Congo Red Dye Using Acid Modified Umuahia Clay: Modeling and Optimization Analysis. *Nigerian Research Journal of Engineering and Environmental Sciences http://doi.org/10.5281/zenodo.12599888*

Onukwuli O.D, Nnaji P.C, Menkiti M.C, Anadebe V.C, Oke E.O, Ude C.N, Ude C.J, Okafor N.A 2021. Dual-purpose optimization of dye-polluted wastewater decontamination using bio-coagulants from multiple processing techniques via neural intelligence algorithm and response surface methodology. Journal of the Taiwan Institute of Chemical Engineers 125, 372- 386. https://doi.org/10.1016/j.jtice.2021.06.030.

Othmani B, Rasteiro M. G, Khadhraoui M. 2020. Toward green technology: a review on some efficient model plant-based coagulants/flocculants for freshwater and wastewater remediation. Clean Technologies and Environmental Policy 22(2) DOI: 10.1007/s10098-020-01858-3

Samal K, Mahapatra S, and Ali Md H 2022 Pharmaceutical wastewater as emerging contaminants (ec): treatment technologies, impact on environment and human health. Energy nexus volume 6. https://doi.org/10.1016/j.nexus.2022.100076

Sibiya, N. P, Rathilal S, and Tetteh, E. K. 2021 Coagulation Treatment of Wastewater: Kinetics and Natural Coagulant Evaluation. Molecules. 26(3):698. doi.org/10.3390/molecules26030698

Varsani V, Vyas S. J, and Dudhagara D. R. 2022 Development of bio-based material from the Moringa oleifera and its bio-coagulation kinetic modeling–A sustainable approach to treat the wastewater. Heliyon 8 e10447. https://doi.org/10.1016/j.heliyon.2022.e10447

Venkatesh P. M, and Karthikeyan R; 2018 Alexandria Engineering Journal 57:3019–3032. https://doi.org/10.1016/j.aej.2018.05.002.

Vijayan D. S, Mohan A, Nivetha C, Sivakumar V, Devarajan P, Paulmakesh A, and Arvindan S. 2022 "Treatment of Pharma Effluent using Anaerobic Packed Bed Reactor," Journal of Environmental and Public Health, vol. 2022, Article ID4657628, 6 pages, 2022.